



# Channel head locations with respect to geomorphologic thresholds derived from a digital elevation model: A case study in northern Thailand

James P. McNamara <sup>a,\*</sup>, Alan D. Ziegler <sup>b</sup>, Spencer H. Wood <sup>a</sup>, John B. Vogler <sup>c</sup>

<sup>a</sup> Department of Geosciences, Boise State University, Boise, ID 83725, USA

<sup>b</sup> Geography Department, University of Hawaii Manoa, Honolulu, HI 96822, USA

<sup>c</sup> Research Program, Environmental Studies, East-West Center, Honolulu, HI 96848, USA

## Abstract

The shape of a catchment is controlled by the interplay of different erosion processes acting within the catchment. It is therefore possible to assess dominant erosion processes, and geomorphologic thresholds that spatially separate those processes, by evaluating catchment form. In this paper, geomorphologic thresholds are detected in a digital elevation model of the Pang Khum Experimental Watershed in northern Thailand and compared to the locations of field mapped channel heads. The intersection of thresholds in the slope-area relationship, the probability distribution of drainage areas, and the probability distribution of energy index produce distinct domains in slope-area space that partition the landscape according to erosion mechanisms. All mapped channel heads plot higher than an energy threshold defined by the product of slope and the square root of drainage area. Above this threshold different types of channel heads are partitioned by independent slope or drainage area thresholds. For example, channel heads formed at groundwater seeps plot higher than a drainage area threshold, independent of slope. Channel heads that originate from landslides and overland flow erosion plot higher than a slope threshold, independent of drainage area. It is our interpretation that the channel heads that did not initiate at groundwater seeps were affected by human disturbance (forest conversion for swidden-based agriculture), as they tend to lay above seeps on highly disturbed hillslopes. This paper explores relationships between the shape of a catchment as defined by a digital elevation model and the distribution of mapped channel heads. These relationships serve as a first-order means to identify locations of potentially unstable areas in a landscape, thereby providing a basis to assess the potential impacts of future catchment disturbances.

© 2005 Elsevier B.V. All rights reserved.

**Keywords:** DEM; GIS; PKEW; Slope-area; Cumulative area distribution; Stream power; Land-cover change; Landslides; Surface erosion

## 1. Introduction

The three-dimensional shape of a catchment develops as erosion works to maintain dynamic equilibrium between landscape properties and the prevailing climate (e.g., Strahler, 1952). Modifications to landscape properties can cause portions of the catchment to seek new equilibrium forms, which may result in accelerated surface erosion, mass wasting, and the ensuing enhanced sediment delivery from uplands to aquatic ecosystems. Important management goals in multi-use watersheds include (1) identifying catchment locations that are particularly sensitive to landslides and surface erosion; and (2) understanding how human activity influences these processes. Initially, one must understand the dominant landscape-shaping processes before any land-management decisions are made.

Continuous monitoring of active erosion processes, however, is beyond the resources of many investigations.

The landscape leaves clues to active erosion processes simply through its geomorphologic form. Geographical information system (GIS) toolkits are useful for deriving indices related to geomorphologic form and process from digital elevation models (DEM), thereby complementing field survey data, which is typically difficult and costly to obtain. Spatial changes in form can demarcate geomorphologic thresholds that separate different erosion mechanisms such as boundaries between areas dominated by diffusive erosion (e.g., rain splash and other forms of unchannelized erosion) and incisive erosion that leads to channelization. A geomorphologic threshold is a limit of equilibrium defined by a balance between erosive driving and resisting forces. When these limits of equilibrium, or thresholds, are exceeded due to changes in the driving forces (e.g., slope, climate, rainfall partitioning) or resisting forces (e.g., soil and vegetation characteristics), the landscape is temporarily in disequilibrium and a major response may occur (Ritter et al., 2002). These major

\* Corresponding author. Tel.: +1 208 426 1354; fax: +1 208 426 4061.

E-mail address: jmcnamar@boisestate.edu (J.P. McNamara).

responses are typically accompanied by characteristic changes in form or breaks in scaling properties (Tucker and Bras, 1998). Consequently, we can identify features in the landscape that reside at or near geomorphologic thresholds simply by analyzing landscape form. For instance, the fluvial channel head exists at a geomorphologic threshold between predominately diffusive erosion and predominantly incisive erosion processes. This is a critical point where a transition occurs in how mass and energy are distributed within a catchment. Channel heads are therefore particularly susceptible to changes in land-use that alter surface erosion and landsliding processes.

Changes in catchment form that accompany thresholds may arise due to the existence of common underlying principles that govern catchment evolution (Montgomery and Dietrich, 1988, 1989). Numerous authors have suggested that the tendency for landscapes to evolve under the principles of energy minimization may be the dominant control on catchment form. For example, the building blocks of catchments (i.e., ridges, valleys, flood-plains and channels) are arranged spatially by diffusive and incisive erosion processes so that energy loss is minimized as water travels through and performs work on the landscape (Langbein, 1964; Langbein and Leopold, 1964; Leopold and Langbein, 1962; Montgomery and Dietrich, 1992; Rodriguez-Iturbe et al., 1992a,b). Rodriguez-Iturbe and Rinaldo (1997) used this underlying principle of energy minimization to explain many classic geomorphologic empiricisms that have been observed for decades in river basins, including commonalities in stream number, stream length, and distribution of drainage areas within any given catchment (Horton, 1945; Schumm, 1956). Sun et al. (1996) suggested that the locations of channel heads are also arranged according to the principles of energy minimization. This commonality among river basins provides metrics to evaluate the stability of catchment form, as well as tools to assess the impacts of natural and anthropogenic disturbances on geomorphology.

In this paper, we evaluate the relationships between channel heads and form-based thresholds in the Pang Khum Experimental Watershed (PKEW) in northern Thailand. We use this information to first understand how channel heads are typically formed in the basin, and then interpret the role that changes in land-cover/land-use has had on the basin morphology. This process allows us to identify basin locations that are sensitive to steepland erosion processes, relative to areas of active and projected land-use activities. We determine the location of channel heads, and thereby the potential for incisive erosion and landslide initiation, by investigating thresholds in three topographic metrics: (1) the slope-area relationship, (2) the probability distribution of cumulative drainage areas, and (3) the probability distribution of energy index, defined as the product of slope and the square root of drainage area. Background information for each type of threshold precedes each presentation of the respective results in Section 5.

## 2. Study area

Pang Khum village ( $19^{\circ}3'N$ ,  $98^{\circ}39'E$ ), is located within the Samoeng District of Chiang Mai Province, approximately



Fig. 1. The study location near Pang Khum village in northern Thailand.

60 km NNW of Chiang Mai, Thailand (Fig. 1). The work focused on a nearby  $\approx 300$ -ha watershed, of which the 93.7-ha Pang Khum Experimental Watershed (PKEW) is a sub-basin (Fig. 2). PKEW is the site of recent hydrological and geomorphologic investigations of the impacts of roads and land-cover conversion in the uplands of northern Thailand (Ziegler et al., 2004). The larger basin is referred to herein as PKEW Yai. Located in Mae Taeng District, it is a part of the

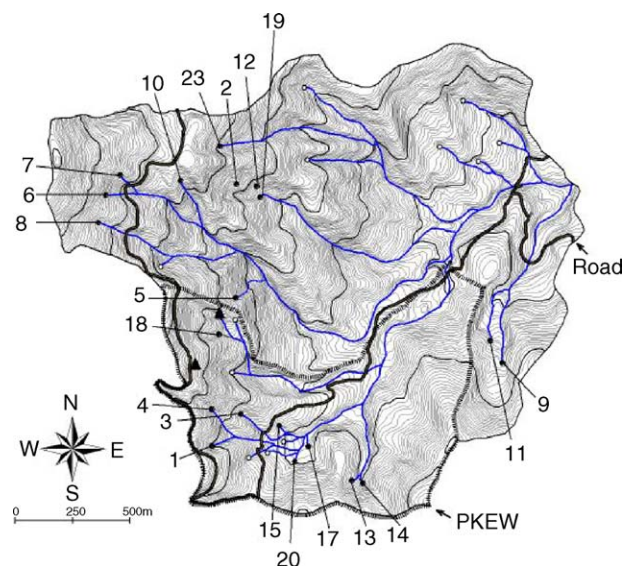


Fig. 2. Map of the PKEW Yai. Bold numbers refer to the 20 mapped channel head locations (filled circles; Table 1). White circles mark the locations of channel heads not surveyed. The two filled triangles mark the locations of two observed landslides without channel heads. The hashed line shows the boundary of the Pang Khum Experimental Watershed (PKEW).

larger Mae Taeng River Basin, which drains into the Ping River, the major tributary to the Chao Praya (Thailand's largest river).

Bedrock is largely muscovite granite, with gneiss being present. Soils are predominantly Ultisols of the Udic moisture regime or Inceptisols occurring on steep upper slopes. The area has a monsoon rainy season that extends from mid-May through October. Analysis of 3 years of data in PKEW indicate that this 5–6 month period accounts for ≈80–90% of an annual total of 1200–2000 mm; annual stream flow (280–825 mm) is 20–40% of the precipitation total. The original pine-dominated forest has been altered by hundreds of years of timber removal and/or swidden cultivation by Karen, Hmong, and recently, Lisu ethnic groups. Some attempts have been made to regenerate the most impacted slopes by planting *Pinus kesiya* Roy. ex Gord. Most lower basin slopes are currently cultivated by Lisu villagers who migrated to Pang Khum from Mae Hong Son Province 2–3 decades ago. Their farming system now resembles a long-term cultivation system with short fallow periods, as opposed to the traditional Lisu long-fallow system (Schmidt-Vogt, 1998). Annual swidden and permanent cultivation activities are similar to those of many groups in northern Thailand (Schmidt-Vogt, 1999). Opium was a prevalent crop before government eradication began about 20–25 years ago. Upland rice and corn are important swidden-based crops; cabbage, cauliflower, onions, garlic, and flowers comprise the cultivated crops.

Approximately 12% of the area in PKEW is agricultural land (cultivated, upland fields, and <1.5-year-old abandoned fields); 13%, fallow land (not used for 1.5–4 years); 31 and 12% are young (4–10 years) and advanced secondary vegetation, respectively; and 31% is disturbed primary forest. PKEW roads comprise 0.5% of the total area; and 70–80% of the total road length drains directly into the stream, typically at intersections between the road and stream channel network (Ziegler et al., 2004). The remaining road runoff often exits unabated onto unprotected hillslopes. With respect to human disturbance, PKEW is representative of PKEW Yai, but road density and the level of agricultural activity are both less in the larger basin. Grazing, forest gathering/hunting, and selected timber removal are, however, similar in both.

### 3. Methods

Geomorphologic thresholds are derived by evaluating distributions of surface slope ( $S$ ) and drainage area ( $A$ ) calculated from a DEM. These variables, coupled with site specific field information, are commonly used to calculate the potential for specific erosion processes to occur for a given storm in a catchment (Dietrich and Montgomery, 1998; Dietrich et al., 1993; Montgomery, 1994; Pack et al., 1998). The variables  $S$  and  $A$  not only control erosion, but erosion leaves its signature on the landscape by modifying these variables. In this study, we use  $S$  and  $A$  in the latter sense as indicators of past erosive actions, rather than as drivers. As such, we avoid the use of site and storm-specific information. We present graphical methods to identify ranges of slopes, areas, or slope-area pairs that are products of different erosion processes. The qualitative nature of this graphical approach is

subject to considerable interpretation if only one metric is used. However, we present an approach in which three topographic metrics of thresholds are plotted together in slope-area space. The resulting accumulation of evidence strengthens the interpretations drawn from individual metrics.

#### 3.1. Field survey

We visited 20 channel heads in June, 2002 in PKEW Yai by hiking to the upper extent of the continuous channel with defined banks (Fig. 2). Channel heads were determined via a global positioning system and/or identifying the position on a 4-m contour topographic map by terrain recognition using a digital altimeter and compass. We used an inclinometer to measure the slope of the surface 30 m above to 30 m below the channel head by laying a rod along the surface, then measuring the slope of the rod relative to horizontal. Local slope was measured similarly as the slope of the surface 2 m above the channel head. Drainage area was determined at each channel head by tracing catchment boundaries from each survey point on the topographic map.

#### 3.2. Slope and area calculations

ArcView GIS (version 3.2) with public domain hydrologic analysis extensions was used to derive slope and drainage area for each pixel in a 4-m DEM of PKEW. The DEM was created from a 4-m contour map that was derived from a 1:50,000 air photo (flight date: 17 December 1995) and georeferenced to known locations on a 1:50,000 topographic map (sheet 4747 III, series L7017, ed. 3-RTSD, Ban Pa Pae; 1992). Slope for each pixel is computed as maximum slope between the pixel and its eight surrounding neighbors in the DEM. Drainage area was computed using the D8 flow accumulation method, for which flow paths connect each pixel to its steepest downslope neighbor. Drainage area is the sum of all pixels along a connected flow path to the pixel of interest multiplied by the area of a pixel ( $16 \text{ m}^2$ ).

### 4. Field survey results

Three types of channel heads in PKEW Yai are those formed by shallow landsliding, erosion by overland flow, and erosion by spring seepage (Table 1, Fig. 3). The processes leading to the development of these channel head types are briefly described as follows:

- Shallow landsliding occurs as a mass failure where channels are typically scoured to bedrock in a catastrophic event beginning at a clearly defined scarp. From a total of four landslides that were documented in the 93.7-ha basin, only two continued as channels and are considered further in this analysis. Both initiated within a few meters below a ridgeline where the concentration of road runoff probably was the triggering mechanism. At the time of the survey, continuous streamflow in both landslide channels began tens of meters below the scarp.

Table 1  
Field-mapped channel heads

| Site | Mechanism             | Drainage area ( $\text{km}^2$ ) | Local slope (m/m) |
|------|-----------------------|---------------------------------|-------------------|
| 1    | Landslide             | 1020                            | 0.70              |
| 2    | Landslide             | 4200                            | 0.97              |
| 3    | Overland flow erosion | 1400                            | 0.84              |
| 4    | Overland flow erosion | 2100                            | 0.58              |
| 5    | Overland flow erosion | 6500                            | 0.72              |
| 6    | Overland flow erosion | 7300                            | 0.71              |
| 7    | Overland flow erosion | 11800                           | 0.80              |
| 8    | Overland flow erosion | 25000                           | 0.65              |
| 9    | Overland flow erosion | 73400                           | 0.20              |
| 10   | Seepage erosion       | 5300                            | 0.64              |
| 11   | Seepage erosion       | 5400                            | 0.49              |
| 12   | Seepage erosion       | 5400                            | 0.55              |
| 13   | Seepage erosion       | 5600                            | 0.23              |
| 14   | Seepage erosion       | 5900                            | 0.26              |
| 15   | Seepage erosion       | 10300                           | 0.48              |
| 16   | Seepage erosion       | 20100                           | 0.32              |
| 17   | Seepage erosion       | 25000                           | 0.20              |
| 18   | Seepage erosion       | 25800                           | 0.22              |
| 19   | Seepage erosion       | 29900                           | 0.55              |
| 20   | Seepage erosion       | 32000                           | 0.33              |

- Erosion by overland flow begins as numerous discontinuous small rills converge to form a continuous channel. Water may or may not be present in the channel at the point of initiation, but the channel has clearly defined banks. All seven of the channels that originated by overland flow erosion occurred on slopes where the original forest cover had been cleared some time in the recent past.
- Seepage erosion occurs at clearly defined groundwater springs located at breaks in topography below which are low-lying valleys; and they are typically obscured by dense vegetation, particularly groves of banana palms. Continuous discharge from the springs forms channels that support perennial streams.

Each channel head type occurs over a wide range of drainage areas and in relatively distinct but overlapping fields in slope-

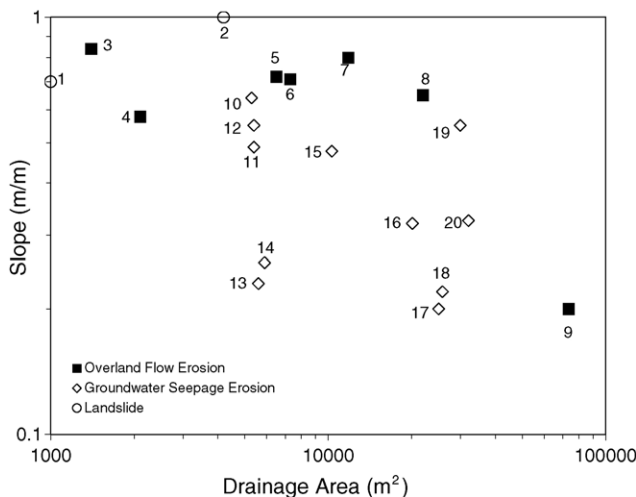


Fig. 3. Channel heads mapped in PKEW Yai. Numbers posted next to symbols refer to Table 1.

area space (Fig. 3). In general, landslide-related heads occurred on steep slopes ( $>0.65 \text{ m m}^{-1}$ ) with comparatively small drainage areas ( $<4500 \text{ m}^2$ ). All but one channel head created by overland flow occurred on steep slopes ( $\geq 0.58 \text{ m m}^{-1}$ ), but over a wide range of drainage areas (1000–70,000  $\text{m}^2$ ). Heads originating from spring seepage erosion occurred at relatively low slopes ( $<0.50 \text{ m m}^{-1}$ ) and for large drainages areas ( $>4500 \text{ m}^2$ ).

## 5. Geomorphologic thresholds

### 5.1. Slope-area relationship

#### 5.1.1. Background

The variables  $S$  and  $A$  are at once both drivers of erosion processes and descriptors of the landscapes response. Relationships between  $S$  and  $A$  can provide critical information regarding the distribution of various erosion processes across the landscape. For example, Flint (1974) reported that the slope of fluvial channels typically scales with drainage area according to:

$$S \sim A^{-\theta} \quad (1)$$

where  $\theta$  is a scaling exponent typically between 0.2 and 0.6. Eq. (1) cannot apply across all scales as it implies an infinite slope as the drainage area approaches zero. Whereas Eq. (1) implies explicitly that slope decreases with increasing drainage area for fluvial channels, slope tends to increase with increasing drainage area on hillslopes. Tarboton et al. (1992), therefore, reasoned that if slope is plotted against drainage area for each point of a catchment DEM,  $\partial S/\partial A$  should be positive in low drainage areas of hillslopes and negative in the higher drainage areas of channels. Tarboton et al. (1992) further claimed that the plot location where  $\partial S/\partial A$  changes from positive to negative (slope-area turnover) is a threshold that should represent the mean drainage area required before channels form.

Willgoose et al. (1991) suggested that the slope-area turnover occurs where diffusive erosion transitions to incisive erosion. This idea has been used as the basis for the commonly accepted method of assigning a threshold drainage to distinguish between hillslopes and channels in DEMs for hydrologic modeling. Montgomery and Foufoula-Georgiou (1993), however, suggested that this threshold drainage area at the slope-area turnover represents the transition from convex hillslopes to concave valleys and that the channel head typically lies somewhere down-valley depending on the local slope. Tucker and Bras (1998) showed through numerical experimentation with a drainage basin evolution model that different erosion processes imprint characteristic signatures on slope-area plots. Turnovers and inflections in slope-area space therefore reveal threshold drainage areas, slopes, and/or slope-area pairs at scales where important transitions occur in a catchment.

#### 5.1.2. Results

A slope-area plot for the PKEW Yai DEM (Fig. 4) can be divided into four drainage area regions separated by thresholds

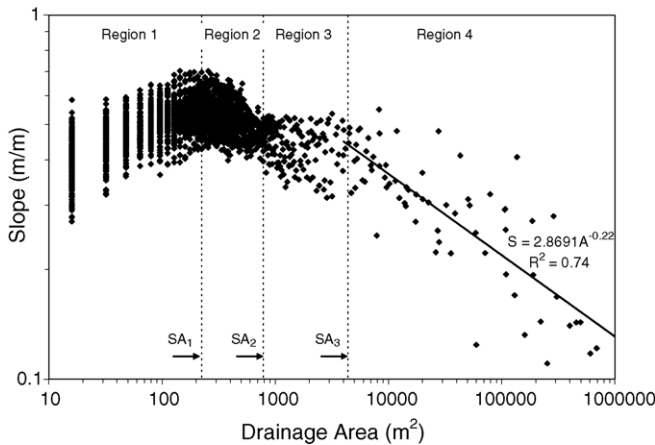


Fig. 4. DEM derived slope-area plot of PKEW Yai. Each point represents the average slope ( $S$ ) for a bin of 100 drainage areas ( $A$ ). Region labels refer to this figure only.

$SA_1$  at  $225 \text{ m}^2$ ,  $SA_2$  at  $800 \text{ m}^2$ , and  $SA_3$  at  $4500 \text{ m}^2$ . In Region 1 slope increases with drainage area until the characteristic slope-area turnover is reached at threshold  $SA_1$ . This log-linear relationship implies the existence of convex topography that is typically controlled by diffusive erosion processes, such as rain splash, soil creep or sheetwash, which tend to round or smooth the landscape (e.g., Hancock, 2005). In Region 2 slope decreases with drainage area, which implies concave topography, until  $SA_2$  is reached. In Region 3 the slope-area relationship resembles the characteristic shape that pore-pressure activated landsliding produces in the Tucker and Bras (1998) model. Slope remains relatively constant near 0.52 (threshold  $S_1$ ) until  $SA_3$  is reached. In Region 4 slope decreases with drainage area according to a power law with an exponent of  $-0.22$ , which is within the expected range for fluvial channels reported by Flint (1974).

## 5.2. Cumulative area distribution

### 5.2.1. Background

The cumulative area distribution (CAD) is constructed by arranging all drainage areas,  $A$ , in a catchment in numerical order and computing the probability of exceedence,  $P(A > A^*)$ , for any given value,  $A^*$ . The shape of a plot of  $P(A > A^*)$  versus  $A^*$  (Fig. 5) is controlled by the convergence patterns of flow paths. Like the slope-area relationship, the CAD for a catchment can therefore show drainage areas where transitions occur in the arrangement of flow paths such as at the hillslope to valley bottom transition, or the transition from unchannelized to channelized terrain at the channel head. In this section we show that each transition in the CAD (Fig. 5) corresponds to changes in the slope-area relationship (Fig. 4). However, these connections between the two analyses are somewhat different than those reported in other studies (Perera and Willgoose, 1998; Hancock, 2005).

It has been suggested that a CAD typically has three regions (Moglen and Bras, 1995; Perera and Willgoose, 1998; Hancock, 2005). Region 1, covering low drainage areas, is typically non-linear in log-log space and is often shaped like an

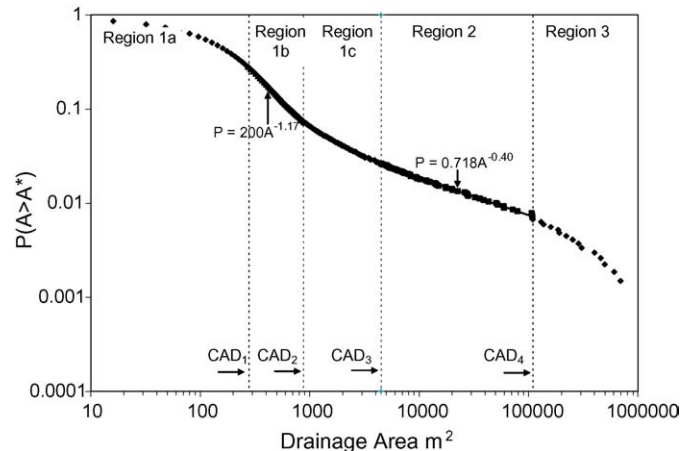


Fig. 5. Cumulative area distribution (CAD) of PKEW Yai derived from a 4-m resolution DEM. The boundaries for the log-log linear Regions 1b and 2 were detected by selecting points at high drainage areas ( $A$ ) clearly within the region and incrementally extending power functions to low drainage areas until the  $r^2$  value decreased. Region labels refer to this figure only.

“S” going from convex to concave, and is considered to represent drainage areas subject to predominantly diffusive erosion (Hancock and Willgoose, 2001). Region 2, which covers intermediate drainage areas, is typically linear in log-log space and is thought to represent the fluvial channel regime subject to incisive erosion. Rodriguez-Iturbe et al. (1992a) reported that the exponent of a power law distribution describing CAD Region 2 tends to be similar and near  $-0.43$  for all fluvial networks, owing to common underlying principles governing the evolution of channel networks. The drainage area where a transition from a non-linear to linear CAD in log-log space should therefore represent the transition from diffusive to incisive erosion, or beginning of the fluvial channel network. A third CAD region typically occurs at large drainage areas where tributaries joining the main channel cause large step increases in drainage area. The limited number of DEM points for these large drainage areas often make interpretations difficult.

Perera and Willgoose (1998) reasoned that because both the slope-area relationship and the CAD display thresholds that represent a transition from diffusive hillslopes to incisive channels, those thresholds should occur in both relationships at similar drainage areas. Specifically, they stated that the beginning of CAD Region 2 should correspond with the slope-area turnover. This notion agrees with the slope-area interpretations of Tarboton et al. (1992) and Willgoose et al. (1991), but disagrees with the ideas presented by Montgomery and Foufoula-Georgiou (1993) that channel head incision occurs at drainage areas greater than where the slope-area turnover occurs. Close inspection of the data presented by Perera and Willgoose (1998) from a catchment in Australia, however, reveals that the beginning of their CAD Region 2 is not coincident with the slope-area turnover as they report, but actually occurs at a greater drainage area; and the slope-area turnover occurs within CAD Region 1. Visual inspection of the Hancock (2005) data for a different Australian catchment also reveals that a turnover in the slope-area relationship occurs

within CAD Region 1—and not at the beginning CAD Region 2 as reported. The results for an arctic Alaskan catchment similarly showed the slope-area turnover occurring in CAD Region 1 (McNamara et al., 1999). In all these cases, if Region 1 is viewed as an “S”, the slope-area turnover occurs at the beginning of an apparent log-log linear region that separates convex and concave regions. Collectively, the Alaskan data and the reinterpretations of the Australian data support the idea presented by Montgomery and Foufoula-Georgiou (1993) that the slope-area turnover represents the transition from convex to concave topography and that the fluvial channel network demarcated by CAD Region 2 begins at somewhat larger drainage areas.

### 5.2.2. Results

Herein we identify five regions in the CAD rather than the three that are typically defined (e.g., Perera and Willgoose, 1998; Hancock, 2005). For simplicity and cross-comparison with other studies we refer to these regions as 1a, 1b, 1c, 2, and 3 (Fig. 5). Regions 1a, 1b and 1c make up the three components of the “S” shaped Region 1 reported by Hancock and Willgoose (2001).

Region 1a is convex in log-log space before a transition to a log-log linear section beginning at threshold CAD<sub>1</sub> at drainage area 270 m<sup>2</sup>. Note that CAD<sub>1</sub> is similar to the drainage area at the turnover in the slope-area relationship (SA<sub>1</sub> at 225 m<sup>2</sup>; Fig. 4). Region 1b is log-log linear until threshold CAD<sub>2</sub> at approximately 880 m<sup>2</sup>, similar to SA<sub>2</sub>. The exponent of a power law function describing Region 1b is -1.17, clearly different from any values reported for fluvial channel networks, which tend to be near -0.43. This suggests that although there is a change in the aggregation structure of flow paths between Regions 1a and 1b, Region 1b is still not in the fluvial channel network.

CAD Region 1c is concave in log-log space and is bounded by thresholds CAD<sub>2</sub> and CAD<sub>3</sub>, which are essentially identical to the thresholds bounding slope-area Region 3 from Fig. 4. In Section 5.1.2 we suggested that this region resembles the shape of a slope-area relationship that arises when pore-pressure activated landsliding is the dominant control on landscape morphology.

The beginning of CAD Region 2 at 4500 m<sup>2</sup> corresponds with the beginning of slope-area Region 4 and is log-log linear wherein the exponent of a power law function is -0.40, which is close to the universal value of -0.43 reported by Rodriguez-Iturbe et al. (1992a). This suggests that CAD Region 2 represents the transition to the fluvial channel network as reported by numerous other authors (Hancock, 2005; Perera and Willgoose, 1998; Rodriguez-Iturbe et al., 1992a; Willgoose et al., 1991). Note that the beginning of CAD Region 2 at 4500 m<sup>2</sup> does not correspond to the slope-area turnover at 225 m<sup>2</sup>. This clear distinction confirms that the two thresholds do not represent the same transitions, which supports our previous conclusion that the slope-area turnover represents a transition from convex to concave topography, but is still in the diffusive erosion regime. This finding agrees with the data presented in numerous other studies (Hancock, 2005; McNamara et al., 1999; Perera and Willgoose, 1998), although it does not necessarily agree with the interpretations of those studies as explained in Section 5.2.1.

CAD Region 3 begins at 110,000 m<sup>2</sup>. The limited number of DEM points for these large drainage areas make interpretations difficult, as suggested in Section 5.2.1.

### 5.3. Distribution of energy index

#### 5.3.1. Background

Catchments are dissipative systems in that energy is released as precipitation travels through the catchment and performs work on the landscape. Energy dissipation in river systems is equivalent to stream power. Stream power per unit flowpath length,  $\Omega$ , is defined as

$$\Omega = Q\rho gm \quad (2)$$

where  $Q$  is the water discharge,  $\rho$  the density of water,  $g$  the gravitational acceleration, and  $m$  is the slope of the energy grade line.

If we assume that  $\rho$  and  $g$  are spatially constant, that discharge scales linearly with drainage area ( $A$ ), and that the energy grade line is parallel to the land surface slope ( $S$ ), stream power, and therefore energy dissipation, can be represented by the product of  $A$  and  $S$ . Variations of this slope-area product have been called stream power index (Moore et al., 1993) and contribution area index (Fontana and Marchi, 2003). In one derivation of the stream power index, Moore et al. (1993) used the specific catchment area:  $A$  divided by a unit contour width. Fontana and Marchi (2003) used the square root of  $A$  to more closely relate their contribution area index to widely used equations of erosion potential; they used their index to identify sediment sources, deposition zones and channel heads. Using principles of energy minimization, Rodriguez-Iturbe et al. (1992a) reasoned that the probability distribution of energy dissipation in a catchment is proportional to the square root of drainage area, and showed that if energy dissipation is computed for each point in a catchment DEM, the probability distribution tends to obey a power law similar to the CAD (Rodriguez-Iturbe et al., 1992a). Thresholds in energy dissipation can therefore be detected by changes in the exponent of a power law distribution of  $A^{0.5}$ .

In this study, we define an energy index (EI) as the product of  $A^{0.5}$  and  $S$ :

$$EI = A^{0.5}S \quad (3)$$

Channel heads occur when a spatial readjustment occurs in the balance between driving forces that cause erosion (e.g., overland flow) and resisting forces that inhibit erosion (viz. soil strength). We can therefore expect different distributions of energy dissipation between channelized and unchannelized terrain or at other points in the channel network where important adjustments occur.

#### 5.3.2. Results

The energy index distribution (EID) for PKEW Yai displays three clear regions (Fig. 6). Region 1 is convex in log-log space. A threshold EID<sub>1</sub> at a value of 14 marks the beginning of a log-log linear Region 2. Region 2 clearly ends at a value of EID<sub>2</sub> = 87. When these thresholds are mapped into slope-area

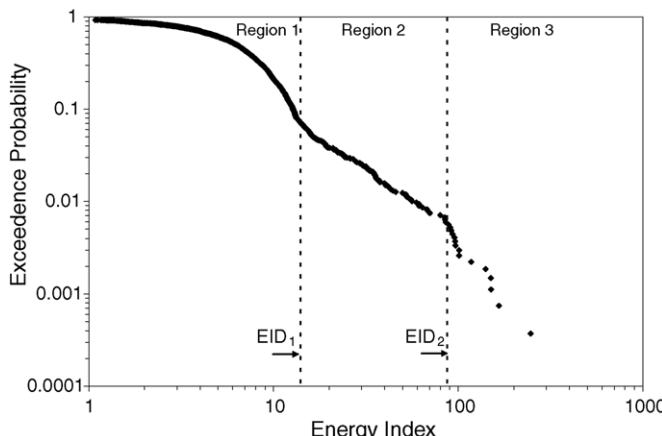


Fig. 6. Probability distribution of the energy index for PKEW Yai. Region labels refer to this figure only.

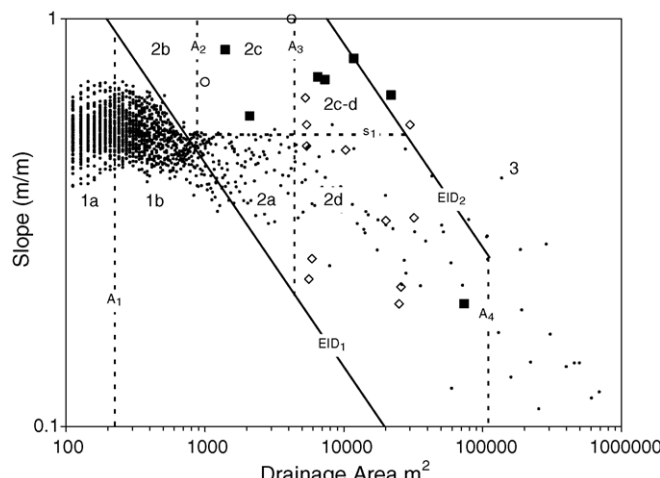


Fig. 7. Intersection of DEM-derived thresholds from Figs. 4–6 in slope-area space. Thresholds are labeled on each line while fields are labeled within the space of each field. Area thresholds represent the average of similar CAD and SA thresholds (from Figs. 4 and 5). Symbols represent the field-mapped channel heads shown in Fig. 3. Small black points are the average slope for a bin of 100 drainage areas (Fig. 4). Field mapped channel heads overlap with raw unaveraged DEM points (not shown). Space is divided into three primary domains by the EID thresholds (solid lines); these domains are further subdivided by the area and slope thresholds (dashed lines).

space they form cross-cutting lines that separate the slope-area plot into three regions (Fig. 7). These lines illustrate the notion that energy thresholds can be viewed as slope-dependent area thresholds. We interpret these energy thresholds with respect to other thresholds and channel heads in Section 6.

## 6. Discussion

### 6.1. Geomorphologic thresholds and channel head formation in PKEW

The overlaps of thresholds in the slope-area relationship, the cumulative area distribution, and the distribution of the energy index form several domains in slope-area space (Fig. 7). Because nearly all mapped channel heads exist between EID<sub>1</sub>

and EID<sub>2</sub>, we identify three primary stability *domains* that are defined by the EID thresholds (cross-cutting lines). Additionally we define seven sub-domains that are determined by drainage area (vertical lines) and slope (horizontal line) thresholds. Area thresholds represent the average of the similar CAD and SA thresholds from Figs. 4 and 5 (e.g., CAD<sub>1</sub> and SA<sub>1</sub> are averaged to produce A<sub>1</sub> in Fig. 7).

#### 6.1.1. Domain 1: hillslopes and unchannelled valleys

The absence of channel heads in Domain 1 suggests that the energy at any point is not sufficient to sustain incisive erosion. Threshold A<sub>1</sub> occurs at the slope-area turnover (Fig. 4) and at a change in the aggregation structure of flow paths (Fig. 5). Slope-area relationships in Domains 1a and 1b suggest that the landscape should be convex and concave, respectively. The contour lines on Fig. 8 show that Domain 1a is composed primarily of divergent topography characteristic of convex hillslopes, while Domain 1b is composed of planar or convergent topography. This supports the suggestion in Section 5.2 that the threshold drainage area CAD<sub>1</sub> and the slope-area turnover at SA<sub>1</sub> define the transition between convex hillslopes and concave valleys, but they do not demarcate the transition from diffusive to incisive erosion process dominance. The threshold A<sub>2</sub> is truncated at EID<sub>1</sub> because it is related to landsliding and has no meaning in Domain 1.

#### 6.1.2. Domain 2: channel initiation

All except two channel heads occur in Domain 2. The two outlying channel heads do however exist close to the threshold EID<sub>2</sub> in Domain 3. Channel heads with low EID indices align close to and higher than EID<sub>1</sub> supporting the suggestion that this threshold represents the minimum energy required to initiate incisive erosion. EID<sub>1</sub> can be viewed as a slope-dependent drainage area threshold. However, there is not a significant relationship between slope and area for field mapped channel heads as other researchers have reported (e.g., Montgomery and Dietrich, 1988). Instead, higher than EID<sub>1</sub>, area and slope thresholds define partitions between the different types of channel heads. For example, many channel heads formed by groundwater springs are aligned with A<sub>3</sub>, independent of slope. Landslides and overland flow channel heads, with one exception, plot higher than S<sub>1</sub> independent of drainage area.

Because channel heads are distributed throughout Domain 2, it is clear that channel initiation does not occur at any one discrete threshold. Local controls such as vegetation, variable soil cohesion, and divergent flow paths at subgrid scales can produce variable erosion susceptibility within each domain. The result is that thresholds represent boundaries within which transitions in process dominance occur.

Domain 2a contains no channel heads, but it plots higher than the energy threshold for incisive erosion. Even though the total energy may be sufficient for incision, neither slope nor drainage area appear sufficient to trigger specific incision mechanisms.

Although Domain 2b exists higher than the energy threshold for channel formation, it also contains no channel heads. It

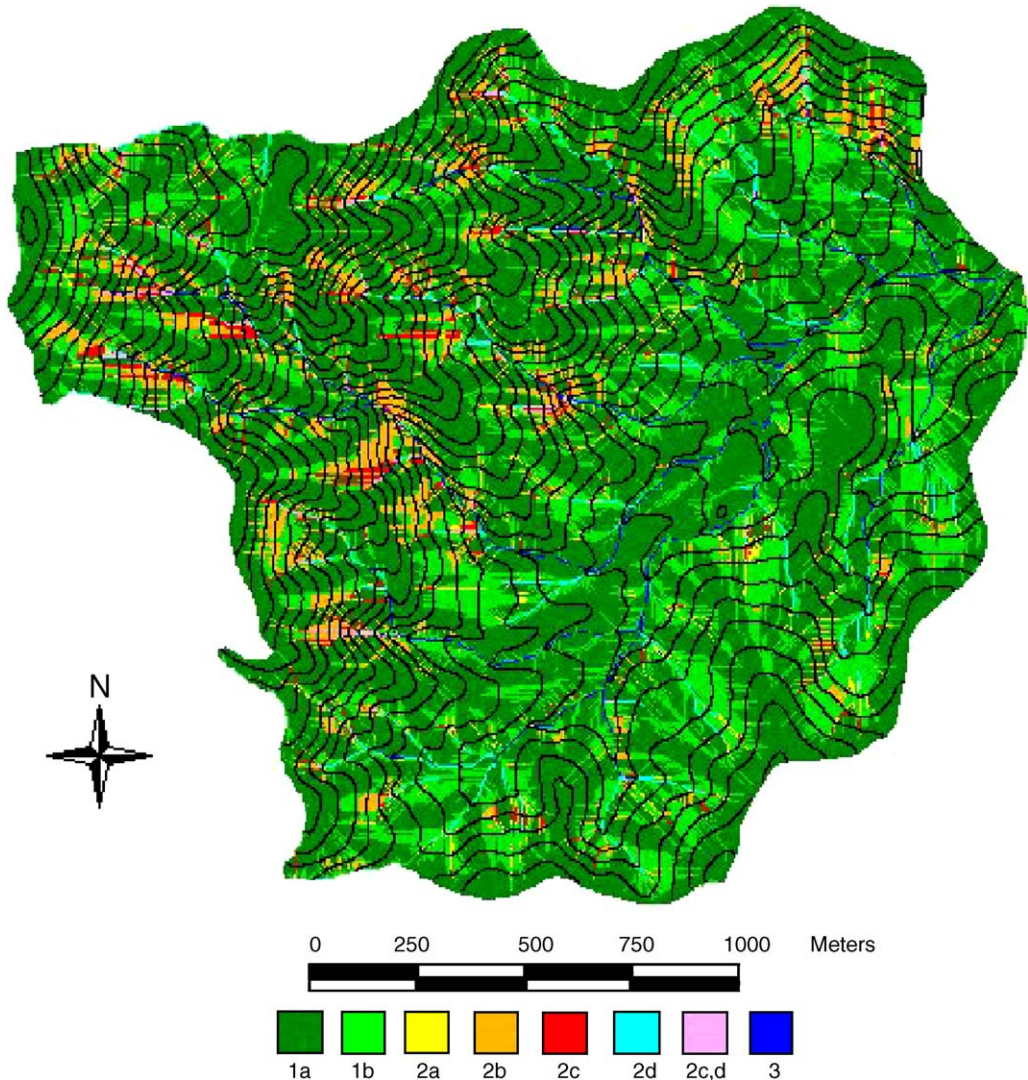


Fig. 8. Distribution of stability domains corresponding to Fig. 7 in Pang Khum Yai.

exists higher than a slope threshold, but below the drainage area threshold  $A_2$ . No landslides were observed in this domain, but it is possible that landslides could occur on the very steep slopes and low drainage areas.

Domain 2c lies higher than slope threshold  $S_1$  and drainage area threshold  $A_2$ , and extends to EID<sub>2</sub>. The relatively constant slope with drainage area, similar to the characteristic slope-area shape that [Tucker and Bras' \(1998\)](#) model predicts, should occur for catchments dominated by pore-pressure activated landsliding. This model also predicts a critical drainage area for landsliding. The occurrence of landslides in Domain 2c suggests that drainage area threshold  $A_2$  could be that critical drainage area.

All but one overland flow channel head plots higher than  $S_1$  independent of drainage area across Domain 2c. It is worth repeating that all of these overland flow channel heads occur on previously disturbed sites.

Field 2d exists higher than the threshold drainage area  $A_3$  and overlaps above  $S_1$  with Domain 2c. All groundwater

seepage channel heads plot higher than this threshold; half plot very close to it. The slope-area relationship ([Fig. 4](#)) and the CAD ([Fig. 5](#)) for drainage areas higher than the threshold  $A_3$  possess properties common to fluvial channel networks as discussed in Section 5 (i.e., the exponent of Eq. (1) is  $-0.22$  and the exponent of a power law function describing the CAD is  $-0.4$ ). The beginning of this spring-fed channel network therefore exists at an important transition in the distribution of mass (drainage area) and energy dissipation (stream power) in the catchment.

#### 6.1.3. Domain 3: fluvial channel network

Whereas Domain 2 is transitional and channel heads may or may not occur depending upon local conditions, Domain 3 is the unequivocal fluvial regime. EID<sub>2</sub> represents an energy state above which unchanneled terrain cannot exist. Threshold  $A_4$  could represent a transition to drainage areas where channels will exist independent of slope—e.g., in broad, essentially flat valley bottoms that are low in the channel network.

## 6.2. Influence of land-use/land-cover on channel head locations

The surveyed channel heads that plot higher than  $S_1$  tend to be created via overland flow erosion or landsliding. The bulk of these locations are on the steep west side of the PKEW, occurring on hillslopes where disturbance (forest conversion, road building, and shifting agriculture) has been great in the last several decades (determined from oral histories and comparison of 1977, 1983, and 1995 aerial photographs with current conditions). In several cases, the channel heads occur at hillslope locations above active groundwater seeps. This suggests that human activity on these steep slopes greater than  $S_1$  has facilitated the upslope migration of the channel heads in recent decades. In doing so, the “footprint” of these heads has shifted up and to the left in the slope-area space shown in Fig. 7. The locations of channel heads 3 and 4 in Domain 2c may have been changed in this manner (cf. Figs. 2 and 3). Both of these channel heads are on converted forest hillslopes. This suggests that current groundwater spring channel heads that plot higher than  $S_1$  may be particularly vulnerable to human disturbance. Channels heads 10, 11, 12, 15, and 19 fall into this category (Figs. 2 and 3).

As another example of how the relationships in Fig. 7 can be used to assess the potential impact of a disturbance, consider the effect that roads have on the hydrology of a catchment. Roads can redirect water from distant parts of a catchment into other domains and artificially increase the drainage area (Montgomery, 1994). This will drive affected points to the right of the figure and increase the energy to enable incisive erosion. A position that naturally lies in the higher slopes of Domain 1 might then shift to Domain 2 and become susceptible to incisive erosion.

## 7. Summary and conclusions

We have related the location of mapped natural- and disturbance-originated channel heads to DEM-derived thresholds in the slope-area relationship, the cumulative area distribution, and the distribution of energy index. The energy index distribution revealed two thresholds that partition slope-area space into three domains. The lower energy domain defines the unchanneled terrain. A threshold in the cumulative area distribution partitions the unchanneled terrain into convex hillslopes to concave valleys. The upper energy domain defines the unequivocal channel network where unchanneled terrain cannot exist. The intermediate energy domain is essentially the channel initiation zone. Because nearly all channel heads exist in the intermediate energy zone, we interpret the lower energy index threshold to be equivalent to a slope-dependent drainage area threshold for channel initiation. However, there is no significant relationship with the slope and area measured at channel heads. Instead, different types of channel heads plot above independent area or slope thresholds. Specifically, channel heads located at groundwater seeps plot higher than a threshold drainage area independent of slope while landslides and overland flow erosion plot higher than a threshold in slope independent of drainage area.

The shape of the slope-area relationship suggests that the form of the overall catchment may be controlled by natural pore-pressure activated landsliding over the long term. Within that structure, groundwater springs begin to emerge at a critical drainage area after a minimum energy is achieved. This critical drainage area marks the beginning of a domain wherein the dominant erosion process transitions from diffusive to incisive. Where that threshold is exceeded, the flow path aggregation pattern resembles a fluvial channel network. However, because all observed landslides and overland flow channel heads occur on disturbed hillslopes, alterations to the hillslopes can cause incisive erosion in the form of landslides and overland flow erosion on steep slopes and lower drainage areas above the perennial spring-fed channel network.

These relationships between field-mapped channel heads and DEM-derived thresholds suggest that the approach presented in this paper offers land managers simple tools to rapidly assess areas of a catchment that may be susceptible to disturbance. When plotted in slope-area space, the combination of the three threshold types provides insight into erosional processes that evaluation of individual thresholds cannot provide. We emphasize, however, that this approach is highly qualitative and that interpretation of thresholds must be guided by sound geologic and hydrogeomorphic concepts. However, we suggest that identifying geomorphologic thresholds and user-derived indices from a DEM can provide a valuable first step to developing more detailed site investigations.

## Acknowledgements

We thank David Montgomery and one anonymous reviewer for their insightful comments that substantially improved the manuscript. We thank Thomas W. Giambelluca, Ross Sutherland, and Mike Nullet, the core members of the PKEW research team, for use of the facility and access to prior data. This work was funded in part by the National Science Foundation USA (grant nos. 9614259, 0000546). The research was approved by the National Research Council Thailand (NRCT), and conducted with permission of the Royal Forest Department (RFD) of Thailand.

## References

- Dietrich, W.E., Montgomery, D.R., 1998. SHALSTAB: a digital terrain model for mapping shallow landslide potential. Report of the National Council for Air and Stream Improvement.
- Dietrich, W.E., Wilson, C.J., Montgomery, D.R., McKean, J., 1993. Analysis of erosion thresholds channel networks and landscape morphology using a digital terrain model. *J. Geol.* 101, 259–278.
- Flint, J.J., 1974. Stream gradient as a function of order, magnitude and discharge. *Water Resour. Res.* 10 (5), 969–973.
- Fontana, G.D., Marchi, L., 2003. Slope-area relationships and sediment dynamics in two alpine streams. *Hydrol. Process.* 17, 77–83.
- Hancock, G.R., 2005. The use of digital elevation models in the identification and characterization of catchments over different grid scales. *Hydrol. Process.* 19, 1727–1749.
- Hancock, G.R., Willgoose, G., 2001. Use of a landscape simulator in the validation of the SIBERIA catchment evolution model: declining equilibrium landforms. *Water Resour. Res.* 37 (7), 1981–1992.

- Horton, R.E., 1945. Erosional development of streams and their drainage basin; hydrophysical approach to quantitative morphology. *Geol. Soc. Am. Bull.* 56, 275–370.
- Langbein, W.B., 1964. Geometry of river channels. *J. Hydraul. Div. Am. Soc. Civ. Eng.* 90 (HY2), 301–312.
- Langbein, W.B., Leopold, L.B., 1964. Quasi-equilibrium states in channel morphology. *Am. J. Sci.* 262, 782–794.
- Leopold, L.B., Langbein W.B., 1962. The concept of entropy in landscape evolution. *USGS Prof. Paper* 500-A.
- McNamara, J.P., Kane, D.L., Hinzman, L.D., 1999. An analysis of arctic channel networks using a digital elevation model. *Geomorphology* 29, 339–353.
- Moglen, G.E., Bras, R.L., 1995. The importance of spatially heterogeneous erosivity and the cumulative area distribution. *Geomorphology* 12 (3), 173–185.
- Montgomery, D.R., 1994. Road surface drainage, channel initiation, and slope stability. *Water Resour. Res.* 30, 1925–1932.
- Montgomery, D.R., Dietrich, W.E., 1992. Channel initiation and the problem of landscape scale. *Science* 255, 826–830.
- Montgomery, D.R., Dietrich, W.E., 1988. Where do channels begin? *Nature* 336, 232–234.
- Montgomery, D.R., Dietrich, W.E., 1989. Source areas, drainage density, and channel initiation. *Water Resour. Res.* 25, 1907–1918.
- Montgomery, D.R., Foufoula-Georgiou, E., 1993. Channel network source representation using digital elevation models. *Water Resour. Res.* 29, 3925–3934.
- Moore, I.D., Turner, A.K., Wilson, J.P., Jenson, S.K., Band, L.E., 1993. GIS and land-surface–subsurface modelling. In: Goodchild, M.F., Parks, B.O., Steyaert, L.T. (Eds.), *Environmental Modelling with GIS*. Oxford University Press, New York, pp. 213–230.
- Pack, R.T., Tarboton, D.G., Goodwin, C.N., 1998. *Terrain Stability Mapping with SINMAP, Technical Description and Users Guide for Version 1.00*, Report Number 4114-0. Terratech Consulting Ltd., Salmon Arm, BC, Canada.
- Perera, H., Willgoose, G., 1998. A physical explanation of the cumulative area distribution curve. *Water Resour. Res.* 34 (5), 1335–1343.
- Ritter, D.F., Kochel, R.C., Miller, J.R., 2002. *Process Geomorphology*, 4th ed. McGraw-Hill, Boston.
- Rodriguez-Iturbe, I., Ijjasz-Vasquez, E., Bras, R.L., 1992a. Power law distributions of mass and energy in river basins. *Water Resour. Res.* 28 (4), 1089–1093.
- Rodriguez-Iturbe, I., Rinaldo, A., Rigon, R., Bras, R.L., Marani, A., Ijjasz-Vasquez, E., 1992b. Energy dissipation, runoff, and the three-dimensional structure of river basins. *Water Resour. Res.* 28 (4), 1095–1103.
- Rodriguez-Iturbe, I., Rinaldo, A., 1997. *Fractal River Basins: Chance and Self-organization*. Cambridge University Press, New York.
- Schmidt-Vogt, D., 1998. Defining degradation: the impacts of swidden on forests in northern Thailand. *Mount. Res. Develop.* 18 (2), 135–149.
- Schmidt-Vogt, D., 1999. Swidden farming and fallow vegetation in northern Thailand. *Geoelectrical Research*, vol. 8. Franz Steiner Verlag, Stuttgart.
- Schumm, S.A., 1956. Evolution of drainage systems and slopes in badlands at Perth Amboy, New Jersey. *Geol. Soc. Am. Bull.* 67 (5), 597–646.
- Strahler, A.N., 1952. Hypsometric (area-altitude) analysis of erosional topography. *Geol. Soc. Am. Bull.* 64, 165–176.
- Sun, T., Meakin, P., Jossang, T., Feder, J., 1996. Possible control of natural channel initiation processes by a minimum energy dissipation rate principle. *Europhys. Lett.* 36 (7), 509–514.
- Tarboton, D.G., Bras, R.L., Rodriguez-Iturbe, I., 1992. A physical basis for drainage density. *Geomorphology* 5, 59–76.
- Tucker, G.E., Bras, R.L., 1998. Hillslope processes, drainage density, and landscape morphology. *Water Resour. Res.* 34 (10), 2751–2764.
- Willgoose, G.R., Bras, R.L., Rodriguez-Iturbe, I., 1991. A physical explanation of an observed link area-slope relationship. *Water Resour. Res.* 27 (7), 1697–1702.
- Ziegler, A.D., Giambelluca, T.W., Sutherland, R.A., Nullet, M.A., Yarnasarn, S., Pinthong, J., Preechapanya, P., Jaiaree, S., 2004. Toward understanding the cumulative impacts of roads in agricultural watersheds of northern Thailand. *Agric. Ecosyst. Environ.* 104, 145–158.